数理解析研究所講究録 1406 巻 2004 年 119-135

Harmonious Representation of PDF's by Two Distinct Tsallis Distribution Functions

T. Arimitsu* (有光敏彦)
Institute of Physics, University of Tsukuba (筑波大 物理)
N. Arimitsu† (有光直子)
EIS, Yokohama National University (横浜国大 環情)

1 Introduction

In this paper, we will show that a harmonious representation of PDF's by means of two distinct Tsallis-type distributions provides us with a description for experimentally or simulationally observed PDF's in the highest accuracy compared with other multifractal model such as the log-normal model [1, 2, 3] and the p model [4, 5]. In order to perform a transparent comparison, the framework of the *multifractal analysis* (MFA) [6, 7, 8, 9, 10, 11, 12, 13, 14, 15, 16, 17, 18, 19, 20] is rephrased in its most sophisticated fashion in which the *tail part* of PDF, giving the probabilities of events larger than its standard deviation, is written down once the multifractal spectrum for the spatial distribution of singularities is specified (see (45) below), whereas the *center part*, giving the probabilities of events smaller than its standard deviation, is assumed to be analyzed by the Tsallis-type PDF for the variable itself [16, 18, 19] (see (47) below). The various PDF's extracted out from the DNS conducted by Gotoh et al. [21, 22], and the PDF of fluid particle accelerations observed by Bodenschatz et al. in their Lagrangian measurement of particle accelerations [23, 24, 25] will be analyzed with the help of the multifractal spectrums for the log-normal, the p model and the harmonious representation.

2 General Framework

2.1 Degree of Singularities

For high Reynolds number $\mathrm{Re} \gg 1$, or for the situation where effects of the kinematic viscosity ν can be neglected compared with those of the turbulent viscosity, the Navier-

*arimitsu@cm.ph.tsukuba.ac.jp
†arimitsu@dnj.ynu.ac.jp

Stokes equation

$$\frac{\partial \vec{u}}{\partial t} + (\vec{u} \cdot \vec{\nabla})\vec{u} = -\vec{\nabla}\left(\frac{p}{\rho}\right) + \nu \nabla^2 \vec{u}, \tag{1}$$

of an incompressible fluid is invariant under the scale transformation [26, 27, 5]

$$\vec{r} \to \lambda \vec{r}, \quad \vec{u} \to \lambda^{\alpha/3}\vec{u}, \quad t \to \lambda^{1-\alpha/3}t, \quad \frac{p}{\rho} \to \lambda^{2\alpha/3}\frac{p}{\rho} \tag{2}$$

where the exponent α is an arbitrary real quantity. The quantities ρ and p represent, respectively, mass density and pressure.

MFA of turbulence rests on the scale invariance of the Navier-Stokes equation for high Reynolds number, and on the assumption that the singularities due to the invariance distribute themselves, multifractally, in physical space. Let us consider the *fluctuation*

$$\delta x_n = |x(\bullet + \ell_n) - x(\bullet)| \tag{3}$$

of a physical quantity x between two points separated by the distance ℓ_n, which satisfies the scaling law

$$|x_n| \equiv \left|\frac{\delta x_n}{\delta x_0}\right| = {\delta_n}^{\alpha\phi/3} \tag{4}$$

with

$$\delta_n = \frac{\ell_n}{\ell_0} = \delta^{-n} \tag{5}$$

where $\delta_n = \delta^{-n}$ ($\delta > 1$, $n = 0, 1, 2, \cdots$). In the following in this paper, we will put $\delta = 2$ that is consistent with the energy cascade model. We are measuring distance by the discrete units

$$\ell_n = \delta_n \ell_0. \tag{6}$$

The non-negative integer n can be interpreted as the *multifractal depth.* However, we will treat it as positive real number in the analysis of experiments. Then, we see that the derivative

$$|x'| = \lim_{n\to\infty} x'_n \tag{7}$$

with the nth difference

$$x'_n = \frac{\delta x_n}{\ell_n} \tag{8}$$

for the characteristic length ℓ_n diverges for $\alpha < 3/\phi$ [28].

Examples are the velocity fluctuation

$$\delta u_n = |u(\bullet + \ell_n) - u(\bullet)| \tag{9}$$

of a component u of velocity field $\vec{u}$, and the *pressure* (divided by the mass density) difference

$$\delta p_n = \left|\frac{p}{\rho}(\bullet + \ell_n) - \frac{p}{\rho}(\bullet)\right|. \tag{10}$$

The scale invariance provides us with

$$|u_n| \equiv \frac{\delta u_n}{\delta u_0} = \delta_n^{\alpha/3} \tag{11}$$

and

$$|p_n| \equiv \frac{\delta p_n}{\delta p_0} = \delta_n^{2\alpha/3} \tag{12}$$

giving, respectively, $\phi = 1$ for the velocity fluctuation and $\phi = 2$ for the pressure fluctuation. The velocity derivative and the fluid particle acceleration may be estimated, respectively, by

$$|u'| = \lim_{n\to\infty} u'_n \tag{13}$$

and by

$$|\vec{a}| = \lim_{n\to\infty} a_n \tag{14}$$

where we introduced the velocity derivative

$$u'_n = \frac{\delta u_n}{\ell_n} \tag{15}$$

and the acceleration (or the pressure derivative)

$$a_n = \frac{\delta p_n}{\ell_n} \tag{16}$$

corresponding to the characteristic length ℓ_n. Note that the acceleration $\vec{a}$ of a fluid particle is given by the substantive time derivative of the velocity:

$$\vec{a} = \frac{\partial \vec{u}}{\partial t} + (\vec{u}\cdot\vec{\nabla})\vec{u}. \tag{17}$$

We see that the velocity derivative and the fluid particle acceleration become singular for $\alpha < 3$ and $\alpha < 1.5$, respectively, i.e.,

$$|u'| \propto \lim_{\ell_n\to 0} \ell_n^{(\alpha/3)-1} \to \infty \tag{18}$$

and

$$|\vec{a}| \propto \lim_{\ell_n\to 0} \ell_n^{(2\alpha/3)-1} \to \infty. \tag{19}$$

The energy-dissipation rate ϵ_n satisfies

$$\frac{\epsilon_n}{\epsilon} = \delta_n^{\alpha-1} \tag{20}$$

due to the scale invariance, giving $\phi = 3$. Therefore, it becomes singular in the limit $n \to \infty$ for $\alpha < 1$, i.e.,

$$\lim_{n\to\infty} \frac{\epsilon_n}{\epsilon_0} \propto \lim_{n\to\infty} \ell_n^{\alpha-1} \to \infty. \tag{21}$$

The real quantity α is introduced in the scale transformation (2) that leaves the Navier-Stokes equation (1) of incompressible fluid invariant with an arbitrary real exponent α when the Reynolds number

$$\mathrm{Re} = \frac{\delta u_{\mathrm{in}} \ell_{\mathrm{in}}}{\nu}, \tag{22}$$

is large. δu_{in} and ℓ_{in} represent, respectively, the rotating velocity and the diameter of the largest eddies in turbulence. The largest size of eddies is, for example, about the order of mesh size of a grid, inserted in a laminar flow, that produces turbulence downstream.

2.2 Singularity Distribution

MFA starts with an assignment of the probability, to find a singularity specified by the strength α within the range $\alpha \sim \alpha + d\alpha$, in the form [5, 10]

$$P^{(n)}(\alpha)d\alpha = \sqrt{\frac{|f''(\alpha_0)||\ln \delta_n|}{2\pi}}\, \delta_n^{1-f(\alpha)}\, d\alpha. \tag{23}$$

Here, $f(\alpha)$ represents an appropriate multifractal spectrum defined in the range $\alpha_{\min} \leq \alpha \leq \alpha_{\max}$. Note that $f(\alpha)$ does not dependent on n because of the scale invariance.

The multifractal spectrum is related to the mass exponent $\tau(\bar{q})$, defined by

$$\left\langle \left(\frac{\epsilon_n}{\epsilon}\right)^{\bar{q}} \right\rangle = a_{3\bar{q}}\, \delta_n^{-\tau(\bar{q})+1-\bar{q}} \tag{24}$$

with

$$a_{3\bar{q}} = \sqrt{\frac{|f''(\alpha_0)|}{|f''(\alpha_{\bar{q}})|}}, \tag{25}$$

through the Legendre transformation [5]:

$$f(\alpha) = \alpha\bar{q} + \tau(\bar{q}) \tag{26}$$

with

$$\alpha = \alpha_{\bar{q}} = -\frac{d\tau(\bar{q})}{d\bar{q}} \tag{27}$$

and

$$\bar{q} = \frac{df(\alpha)}{d\alpha}. \tag{28}$$

The average $\langle \cdots \rangle$ is taken with $P^{(n)}(\alpha)$, and $\alpha_0 = \alpha_{\bar{q}=0} = \langle \alpha \rangle$.

The scaling exponent ζ_m of the mth order velocity structure function, defined by

$$\langle |u_n|^m \rangle \propto \delta_n^{\zeta_m}, \tag{29}$$

is related to the mass exponent by

$$\zeta_m = 1 - \tau\left(\frac{m}{3}\right). \tag{30}$$

This is derived with the help of (11) and (20) as

$$\langle |u_n|^m \rangle = \delta_n^{m/3} \left\langle \left(\frac{\epsilon_n}{\epsilon} \right)^{m/3} \right\rangle = a_m \delta_n^{1-\tau(m/3)}. \tag{31}$$

2.3 Observable Probability Density Functions

The probability $\Pi_\phi^{(n)}(x_n)dx_n$ to find a physical quantity x_n in the range $x_n \sim x_n + dx_n$ is assumed to consist of two parts

$$\Pi_\phi^{(n)}(x_n)dx_n = \Pi_{\phi,\mathrm{S}}^{(n)}(x_n)dx_n + \Delta\Pi_\phi^{(n)}(x_n)dx_n \tag{32}$$

with the normalization

$$\int_{-\infty}^{\infty} dx_n \Pi_\phi^{(n)}(x_n) = 1. \tag{33}$$

The first term represents the contribution by the singular part of the quantity x_n stemmed from the multifractal distribution of its singularities in physical space. This is given by

$$\Pi_{\phi,\mathrm{S}}^{(n)}(|x_n|)\ d|x_n| = \frac{1 - 2\gamma_{\phi,0}^{(n)}}{2}\ P^{(n)}(\alpha)\ d\alpha \tag{34}$$

with the transformation of the variables (4), i.e.,

$$|x_n| = \delta_n^{\phi\alpha/3}. \tag{35}$$

Here, we introduced $\gamma_{\phi,m}^{(n)}$ by

$$2\gamma_{\phi,m}^{(n)} = \int dx_n |x_n|^m \Delta\Pi_\phi^{(n)}(x_n). \tag{36}$$

The second term $\Delta\Pi_\phi^{(n)}(x_n)dx_n$ represents the contribution from the dissipative term in the Navier-Stokes equation, and/or the one from the errors in measurements. The dissipative term has been discarded in the above investigation for the distribution of singularities since it violates the invariance under the scale transformation. The contribution of the second term provides a correction to the first one. Note that we are dealing with the symmetrized part of PDF's by assuming that the large deviation stemmed from the singular first term contributes to symmetric part of PDF's.

Needless to say that each term in (32) is a multiple of two probability functions, i.e., the one to determine the portion of the contribution among two independent origins, and the other to find x_n in the range $x_n \sim x_n + dx_n$. Nore that the values of x_n originated in the singularity are rather large representing intermittent large deviations, and that those contributing to the correction terms are small in comparison with its deviation.

The mth moment of the structure functions for the variable $|x_n|$,

$$\langle\langle |x_n|^m \rangle\rangle = \int_{-\infty}^{\infty} dx_n |x_n|^m \Pi_\phi^{(n)}(x_n), \tag{37}$$

reduces to

$$\langle\langle |x_n|^m \rangle\rangle = 2\gamma_{\phi,m}^{(n)} + (1 - 2\gamma_{\phi,0}^{(n)})\ a_{\phi m}\ \delta_n^{\zeta_{\phi m}} \tag{38}$$

with the corresponding scaling exponents

$$\zeta_{\phi m} = 1 - \tau\left(\frac{\phi m}{3}\right) \tag{39}$$

For $\phi = 1$, $\zeta_{\phi m}$ reduces to the scaling exponents ζ_m of the mth order velocity structure function.

We now derive the PDF, $\hat{\Pi}_\phi^{(n)}(\xi_n)$, defined by the relation

$$\hat{\Pi}_\phi^{(n)}(\xi_n)\ d\xi_n = \Pi_\phi^{(n)}(x_n)\ dx_n \tag{40}$$

or by

$$\hat{\Pi}_\phi^{(n)}(\xi_n)\ d\xi_n = \Pi_\phi^{(n)}(x'_n)\ dx'_n \tag{41}$$

for the variable

$$\xi_n = \frac{x_n}{\sqrt{\langle\langle |x_n|^2 \rangle\rangle}} = \frac{x'_n}{\sqrt{\langle\langle (x'_n)^2 \rangle\rangle}} \tag{42}$$

both of the fluctuation x_n and of the derivative x'_n normalized by their own standard deviations. This PDF is to be compared with the PDF's obtained by observations. The variable is related with α by

$$|\xi_n| = \bar{\xi}_n \delta_n^{\phi\alpha/3 - \zeta_{2\phi}/2} \tag{43}$$

with

$$\bar{\xi}_n = \frac{1}{\sqrt{2\gamma_{\phi,2}^{(n)} \delta_n^{-\zeta_{2\phi}} + \left(1 - 2\gamma_{\phi,0}^{(n)}\right) a_{2\phi}}}. \tag{44}$$

It is reasonable to imagine that the origin of intermittent rare events is attributed to the first singular term in (32), and that the contribution from the second term is negligible. We then have, for $\xi_n^* \le |\xi_n| \le \xi_n^{\max}$ (equivalently, $\alpha_{\min} \le |\alpha| \le \alpha^*$),

$$\hat{\Pi}_\phi^{(n)}(|\xi_n|)\ d|\xi_n| = \Pi_{\phi,\mathrm{S}}^{(n)}(|x_n|)\ d|x_n| = \frac{1 - 2\gamma_{\phi,0}^{(n)}}{2}\ P^{(n)}(\alpha)\ d\alpha \tag{45}$$

with

$$\xi_n^{\max} = \bar{\xi}_n \delta_n^{\phi\alpha_{\min}/3 - \zeta_{2\phi}/2}. \tag{46}$$

Note that $\xi_n^* \sim 1$ as can be seen below when we analyze experiments. This *tail part* represents the large deviations, and manifests itself the multifractal distribution of the singularities due to the scale invariance of the Navier-Stokes equation when its dissipative term can be neglected.

On the other hand, for smaller values, the contribution to the PDF comes, mainly, from thermal fluctuations or measurement error. For smaller values of the variable, $|\xi_n| \le \xi_n^*$

(equivalently, $\alpha^* \leq |\alpha|$), we assume that the PDF has the Tsallis-type structure with a new entropy index q' [16, 18]

$$\hat{\Pi}_{\phi}^{(n)}(\xi_n)d\xi_n = \left[\Pi_{\phi,\mathrm{S}}^{(n)}(x_n) + \Delta\Pi_{\phi}^{(n)}(x_n)\right] dx_n$$
$$= \bar{\Pi}_{\phi}^{(n)} \left\{1 - (1-q')\frac{(\phi + 3f'(\alpha^*))}{2\phi}\left[\left(\frac{\xi_n}{\xi_n^*}\right)^2 - 1\right]\right\}^{1/(1-q')} d\xi_n \tag{47}$$

where

$$\bar{\Pi}_{\phi}^{(n)} = \frac{3(1-2\gamma_{\phi,0}^{(n)})\sqrt{|f''(\alpha_0)|}}{2\phi\bar{\xi}_n\sqrt{2\pi|\ln\delta_n|}}. \tag{48}$$

This *center part* is responsible to smaller fluctuations of the variable, compared with its standard deviation, stemmed from the dissipative term violating the scale invariance. The entropy index q' can be dependent on the distance of two measuring points separated by ℓ_n.

The two parts of the PDF, (45) and (47), are connected at

$$\xi_n^* = \bar{\xi}_n \delta_n^{\phi\alpha^*/3 - \zeta_{2\phi}/2} \tag{49}$$

under the conditions that they have the common value, $\bar{\Pi}_{\phi}^{(n)}$, and the common log-slope, $-(\phi + 3f'(\alpha^*))/\phi\xi_n^*$ there. The value α^* is the smaller solution of

$$\frac{\zeta_{2\phi}}{2} - \frac{\phi\alpha}{3} + 1 - f(\alpha) = 0. \tag{50}$$

The point ξ_n^* has the characteristics that the dependence of $\hat{\Pi}_{\phi}^{(n)}(\xi_n^*)$ on n is minimum for large n (see Fig. 4 in [11]).

With the help of (45) and (47), we obtain $\Delta\Pi_{\phi}^{(n)}(x_n)$, and have the analytical formula

$$2\gamma_{\phi,m}^{(n)} = \frac{K_{\phi,m}^{(n)} - L_{\phi,m}^{(n)}}{1 + K_{\phi,0}^{(n)} - L_{\phi,0}^{(n)}} \tag{51}$$

where

$$K_{\phi,m}^{(n)} = \frac{3\delta_n^{(m+1)\phi\alpha^*/3 - \zeta_{2\phi}/2}}{\phi}\sqrt{\frac{|f''(\alpha_0)|}{2\pi|\ln\delta_n|}}$$
$$\times \int_0^1 dz\ |z|^m \left[1 - (1-q')\frac{\phi + 3f'(\alpha^*)}{2\phi}(z^2-1)\right]^{1/(1-q')} \tag{52}$$

$$L_{\phi,m}^{(n)} = \delta_n\sqrt{\frac{|f''(\alpha_0)||\ln\delta_n|}{2\pi}}\int_{\alpha^*}^{\alpha_{\max}} d\alpha\ \delta_n^{m\alpha\phi/3 - f(\alpha)}. \tag{53}$$

The flatness $F_x^{(n)}$ of the PDF for the variable x_n is given by

$$F_x^{(n)} \equiv \frac{\langle\langle |x_n|^4 \rangle\rangle}{\langle\langle |x_n|^2 \rangle\rangle^2} = \langle\langle \xi_n^4 \rangle\rangle = \frac{2\gamma_{\phi,4}^{(n)} + (1 - 2\gamma_{\phi,0}^{(n)})a_{4\phi}\delta_n^{\zeta_{4\phi}}}{\left[2\gamma_{\phi,2}^{(n)} + (1 - 2\gamma_{\phi,0}^{(n)})a_{2\phi}\delta_n^{\zeta_{2\phi}}\right]^2}. \tag{54}$$

For later convenience, we introduce here the quantity $\xi_{n,0} = \bar{\xi}_n \delta_n^{\phi\alpha_0/3-\zeta_{2\phi}/2}$.

3 Harmonious Representation

In the harmonious representation of MFA, we adopt the Tsallis-type distribution function [7, 8, 9, 10]

$$P^{(n)}(\alpha) = \frac{1}{Z_\alpha^{(n)}} \left[1 - \left(\frac{\alpha - \alpha_0}{\Delta\alpha}\right)^2\right]^{n/(1-q)} \tag{55}$$

with

$$(\Delta\alpha)^2 = \frac{2X}{(1-q)\ln 2}. \tag{56}$$

Here, q is the entropy index introduced in the definitions of the Rényi [29] and the Tsallis entropies [30, 31]. The range of α is $\alpha_{\min} \leq \alpha \leq \alpha_{\max}$ with

$$\alpha_{\min} = \alpha_0 - \Delta\alpha, \quad \alpha_{\max} = \alpha_0 + \Delta\alpha. \tag{57}$$

The normalization condition

$$\int_{\alpha_{\min}}^{\alpha_{\max}} d\alpha \; P^{(n)}(\alpha) = 1 \tag{58}$$

gives the partition function in the form

$$Z_\alpha^{(n)} = \Delta\alpha \; B(1/2, 1 + n/(1-q)) \tag{59}$$

where $B(a, b)$ is the Beta function.

The distribution function (55) is derived by adopting the measure of the Renyi entropy [29] or of the Havrda-Charvat-Tsallis (HCT) entropy [31, 30] with an appropriate constraint. In spite of the different characteristics of the entropies, i.e., extensive and non-extensive, the distribution functions $P^{(n)}(\alpha)$ giving their extremum have the common structure. [1] Note that since the Renyi entropy and HCT entropy reduce to the Boltzmann-Gibbs entropy in the limit $q \to 1$, the probability density function (55) derived from these entropies reduces to the Boltzmann-Gibbs distribution function in the limit.

The multifractal spectrum $f(\alpha)$ is given by [7, 8, 9, 10]

$$f(\alpha) = 1 + \frac{1}{1-q} \log_2 \left[1 - \left(\frac{\alpha - \alpha_0}{\Delta\alpha}\right)^2\right] \tag{60}$$

which, then, produces the mass exponent

$$\tau(\bar{q}) = 1 - \alpha_0 \bar{q} + \frac{2X\bar{q}^2}{1 + \sqrt{C_{\bar{q}}}} + \frac{1}{1-q}\left[1 - \log_2\left(1 + \sqrt{C_{\bar{q}}}\right)\right] \tag{61}$$

[1] Within the present formulation, the decision cannot be pronounced which of the entropies is underlying the system of turbulence.

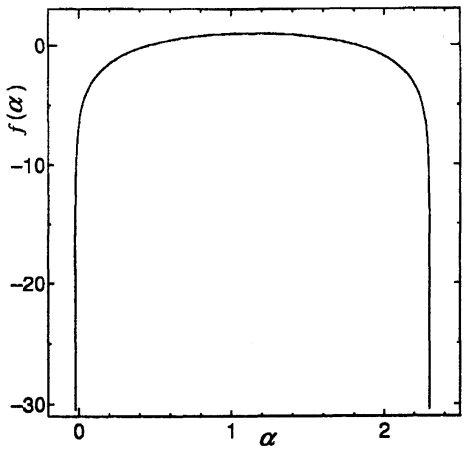

Figure 1: Multifractal spectrum $f(\alpha)$ with $\mu = 0.240$ ($q = 0.391$).

with

$$C_{\bar{q}} = 1 + 2\bar{q}^2(1-q)X \ln 2. \tag{62}$$

The typical shape of the multifractal spectrum and of the generalized dimension $D_{\bar{q}}$ defined through

$$\tau(\bar{q}) = (1-\bar{q})D_{\bar{q}} \tag{63}$$

are given, respectively, in Fig. 1 and Fig. 2.

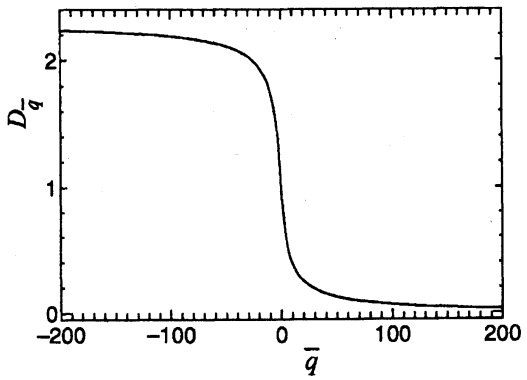

Figure 2: Generalized dimension $D_{\bar{q}}$ with $\mu = 0.240$ ($q = 0.391$).

We have

$$f''(\alpha_{\bar{q}}) = -\frac{\sqrt{C_{\bar{q}}}\left(1+\sqrt{C_{\bar{q}}}\right)}{2X} \tag{64}$$

with

$$\alpha_{\bar{q}} = \alpha_0 - \frac{2\bar{q}X}{1+\sqrt{C_{\bar{q}}}}, \tag{65}$$

hence

$$a_{3\bar{q}} = \sqrt{\frac{2}{\sqrt{C_{\bar{q}}}\left(1+\sqrt{C_{\bar{q}}}\right)}}. \tag{66}$$

The scaling exponents ζ_m for the mth order velocity structure function, defined by (39) with $\phi = 1$, reduce to [7, 8, 9, 10]

$$\zeta_m = \frac{\alpha_0 m}{3} - \frac{2Xm^2}{9\left(1+\sqrt{C_{m/3}}\right)} - \frac{1}{1-q}\left[1 - \log_2\left(1+\sqrt{C_{m/3}}\right)\right]. \tag{67}$$

The formula (67) is independent of n, which is a manifestation of the scale invariance.

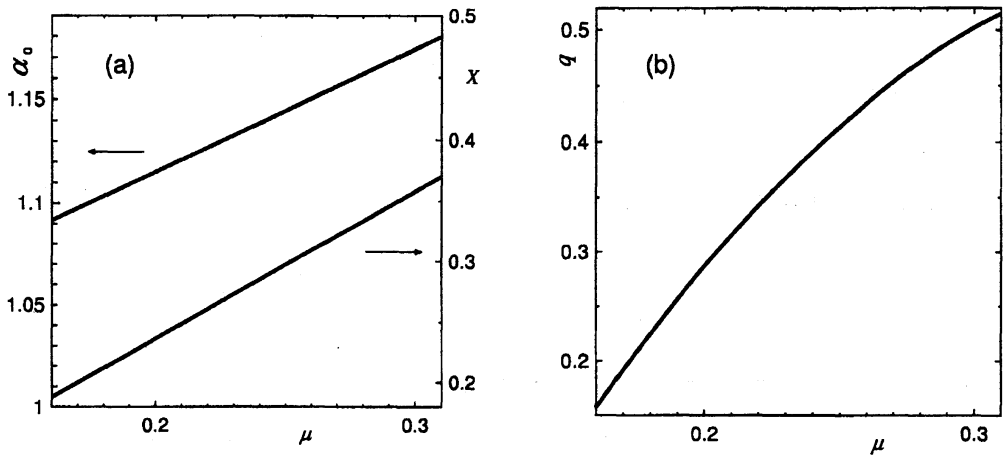

Figure 3: (a) The μ-dependence of α_0 and X. Squares and circles are the points where the self-consistent equations are solved. (b) The μ-dependence of q. Circles are the points where the self-consistent equations are solved.

The dependence of the parameters α_0, X and q on the intermittency exponent μ is determined, self-consistently, with the help of the three independent equations, i.e., the energy conservation:

$$\left\langle \frac{\epsilon_n}{\epsilon} \right\rangle = 1, \quad \text{equivalently,} \quad \tau(1) = 0 \tag{68}$$

the definition of the intermittency exponent μ:

$$\left\langle \left(\frac{\epsilon_n}{\epsilon}\right)^2 \right\rangle = \delta_n^{-\mu}, \quad \text{equivalently,} \quad \mu = 1 + \tau(2) \tag{69}$$

and the scaling relation: [2]

$$\frac{1}{1-q} = \frac{1}{\alpha_-} - \frac{1}{\alpha_+} \tag{70}$$

with $\alpha_\pm$ satisfying $f(\alpha_\pm) = 0$. The average $\langle \cdots \rangle$ is taken with $P^{(n)}(\alpha)$. Within the range $0.13 \leq \mu \leq 0.40$ where most of the experiments are covered, these self-consistent equations are solved, numerically, with respect to μ to give [14]

$$\alpha_0 = 0.9989 + 0.5814\mu, \tag{71}$$

[2]The scaling relation is a generalization of the one derived first in [32, 33] to the case where the multifractal spectrum has negative values.

$$X = 1.198\mu \tag{72}$$

and

$$q = -1.507 + 20.58\mu - 97.11\mu^2 + 260.4\mu^3 - 365.4\mu^4 + 208.3\mu^5. \tag{73}$$

They are given in Fig. 3. It is interesting to compare the first two with the corresponding equations for the log-normal model ($q = 1$) given in senction 4, i.e., $\alpha_0 = 1 + 0.5\mu$ and $X = \mu$.

The explicit form of the PDF (45) for $\xi_n^* \leq |\xi_n| \leq \xi_n^{\max}$ turns out to be

$$\hat{\Pi}_\phi^{(n)}(\xi_n) = \bar{\Pi}_\phi^{(n)} \frac{\bar{\xi}_n}{|\xi_n|} \left[1 - \frac{1-q}{n} \frac{(3\ln|\xi_n/\xi_{n,0}|)^2}{2\phi^2 X |\ln\delta_n|}\right]^{n/(1-q)}. \tag{74}$$

The entropy index q should be unique once a turbulent system with a certain Reynolds number is specified.

4 Log-Normal Model

In the log-normal model [1, 2, 3], one consider the ratio $\epsilon_n/\epsilon_{n-1}$ $(n = 1, 2, \cdots)$ as independent stochastic variables, and apply for $n \gg 1$ the central limit theorem to the summation of their logarithms,

$$\frac{1}{\sqrt{n\sigma^2}} \sum_{j=1}^{n} \ln\left(\frac{\epsilon_j}{\epsilon_{j-1}}\right) = \frac{1}{\sqrt{n\sigma^2}} \ln\left(\frac{\epsilon_n}{\epsilon}\right) = \sqrt{\frac{n}{\sigma^2}}\,(1-\alpha)\ln\delta, \tag{75}$$

to have the Gaussian distribution function

$$P^{(n)}(\alpha) = \sqrt{\frac{n}{2\pi\sigma^2}}\, \mathrm{e}^{-n(\alpha-\alpha_0)^2/2\sigma^2} \tag{76}$$

for the range $-\infty < \alpha < \infty$. Here, we used the scaling relation (20) between ϵ_n and α. Then, we have the multifractal spectrum and the mass exponent in the forms

$$f(\alpha) = 1 - \frac{(\alpha-\alpha_0)^2}{2\sigma^2 \ln\delta} \tag{77}$$

and

$$\tau(\bar{q}) = 1 - \alpha_0\bar{q} + \frac{1}{2}\bar{q}^2\sigma^2\ln\delta, \tag{78}$$

respectively. We see that

$$a_{3\bar{q}} = 1. \tag{79}$$

The dependence of the parameters α_0 and σ on the intermittency exponent μ is determined with the help of the two independent equations, i.e., the energy conservation (68) and the definition of the intermittency exponent μ (69). The parameters are specified by means of μ as

$$\alpha_0 = 1 + \frac{\mu}{2} \tag{80}$$

and

$$\sigma^2 = \frac{\mu}{\ln \delta}. \tag{81}$$

Then, we have

$$f(\alpha) = 1 - \frac{(\alpha - \alpha_0)^2}{2\mu} \tag{82}$$

and

$$\tau(\bar{q}) = (1 - \bar{q}) D_{\bar{q}} \tag{83}$$

with the generalized dimension

$$D_{\bar{q}} = 1 - \mu \bar{q}/2, \tag{84}$$

which are the same as derived in [5]. We know that

$$\alpha_{\bar{q}} = \alpha_0 - \mu \bar{q}. \tag{85}$$

The explicit form of the PDF (45) for $\xi_n^* \leq |\xi_n| < \infty$ is found to be

$$\hat{\Pi}_{\phi}^{(n)}(\xi_n) = \bar{\Pi}_{\phi}^{(n)} \frac{\bar{\xi}_n}{|\xi_n|} \exp\left[-\frac{(3 \ln |\xi_n / \xi_{n,0}|)^2}{2\phi^2 \mu |\ln \delta_n|} \right]. \tag{86}$$

The connection point is given by

$$\alpha^* = \alpha_0 - \frac{\sqrt{3} - 1}{3} \phi \mu. \tag{87}$$

5 P Model

The distribution function $P^{(n)}(\alpha)$ for the p model [4, 5] is specified based on the binomial multiplicative process in the form [6]

$$P^{(n)}(\alpha) = \frac{1}{Z_0^{(n)}} \frac{1}{[2y^y (1-y)^{1-y}]^n} \tag{88}$$

with

$$y = y(\alpha) = \frac{\alpha + \log_2(1-p)}{\log_2[(1-p)/p]} \tag{89}$$

and the partition function

$$Z_0^{(n)} = \sqrt{\frac{\pi}{2n}} \log_2 \left(\frac{1-p}{p} \right) \tag{90}$$

for $n \gg 1$.

The multifractal spectrum is given by

$$f(\alpha) = -\left\{ y(\alpha) \log_2 y(\alpha) + [1 - y(\alpha)] \log_2 [1 - y(\alpha)] \right\}, \tag{91}$$

which leads to the mass exponent

$$\tau(\bar{q}) = \log_2 [p^{\bar{q}} + (1-p)^{\bar{q}}] . \tag{92}$$

We have

$$f''(\alpha_{\bar{q}}) = -\frac{\ln 2}{\{\ln[(1-p)/p]\}^2 y_{\bar{q}}(1-y_{\bar{q}})} \tag{93}$$

with

$$y_{\bar{q}} = y(\alpha_{\bar{q}}) = \frac{p^{\bar{q}}}{p^{\bar{q}} + (1-p)^{\bar{q}}}, \tag{94}$$

$$\alpha_{\bar{q}} = -\frac{p^{\bar{q}} \log_2 p + (1-p)^{\bar{q}} \log_2 (1-p)}{p^{\bar{q}} + (1-p)^{\bar{q}}}, \tag{95}$$

and then we obtain

$$a_{3\bar{q}} = \frac{2\sqrt{p^{\bar{q}}(1-p)^{\bar{q}}}}{p^{\bar{q}} + (1-p)^{\bar{q}}}. \tag{96}$$

We see that, for $p > 1/2$,

$$\alpha_{\min} = -\log_2 p, \tag{97}$$

$$\alpha_{\max} = -\log_2 (1-p). \tag{98}$$

The dependence of p on the intermittency coefficient μ is derived through its definition (69) to give

$$p = \frac{1 + \sqrt{2\mu - 1}}{2}. \tag{99}$$

The explicit form of the PDF (45) for $\xi_n^* \leq |\xi_n| \leq \xi_n^{\max}$ reduces to

$$\hat{\Pi}_\phi^{(n)}(\xi_n) = \bar{\Pi}_\phi^{(n)} \frac{\bar{\xi}_n}{|\xi_n|} \left\{ (1+2\delta y)^{1+2\delta y} (1-2\delta y)^{1-2\delta y} \right\}^{-n/2} \tag{100}$$

with

$$\delta y = y - y_0 = \frac{3 \ln(|\xi_n|/|\xi_{n,0}|)}{\phi \{\log_2[(1-p)/p]\} |\ln \delta_n|}. \tag{101}$$

6 Comparison of Three models

The scaling exponents ζ_m of velocity structure function reported by Gotoh et al. [21] are analyzed in Fig. 4 by the method of the least squares (MLS) with the theoretical formulae of the harmonious representation, of the log-normal model and of the p model, giving, respectively, the values of the intermittency exponent $\mu = 0.240$, 0.217 and 0.249.

In Fig. 5, the PDF's of the velocity fluctuations (closed circles) measured by Gotoh et al. in their DNS at $R_\lambda = 380$ [21] for three different measuring distances, $r/\eta = \ell_n/\eta = 2.38$, 19.0, 1220 from the top set of pairs to the bottom set, are analyzed with the help of the PDF's $\hat{\Pi}^{(n)}(\xi_n)$ of the harmonious representation (solid line) and of the log-normal model (dashed line). Here, $\eta = (\nu^3/\epsilon)^{1/4}$ represents the Kolmogorov scale. The DNS data

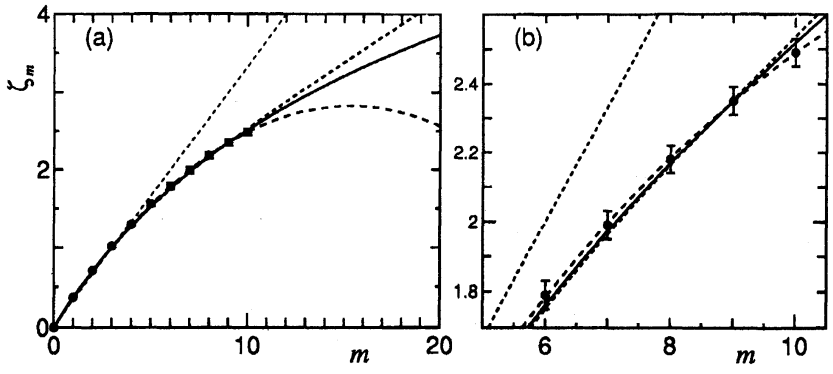

Figure 4: Analysis of the scaling exponents ζ_m of velocity structure function extracted from the DNS conducted by Gotoh et al. by the present theoretical curve (solid line). Those by K41 (dotted line), the log-normal model (dashed line) and the p model (dotted-dashed line) are also shown for comparison.

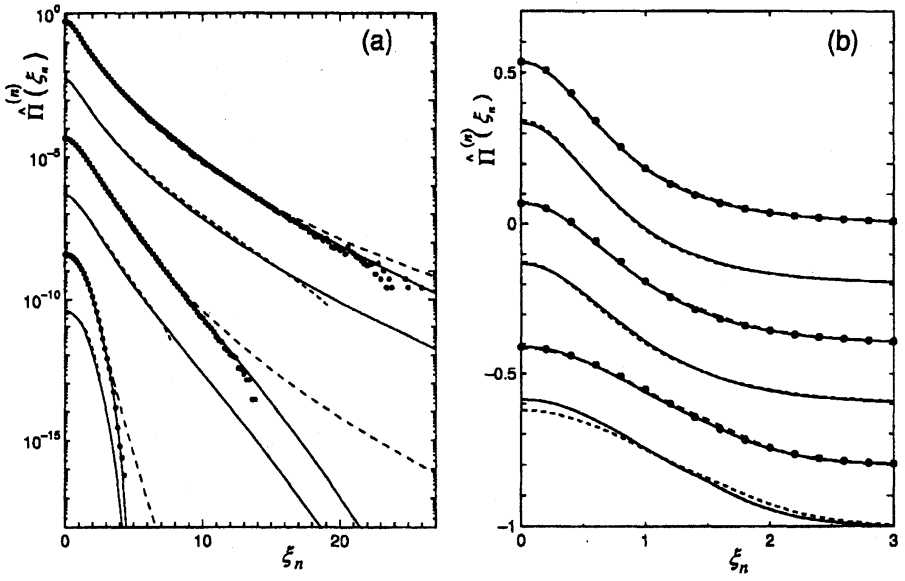

Figure 5: Analyses of the PDF's of the velocity fluctuations (closed circles) for three different measuring distances, observed by Gotoh et al. at $R_\lambda = 380$, with the help of the PDF's $\hat{\Pi}^{(n)}(\xi_n)$ by the harmonious representation (solid line) and by the log-normal model (dashed line) are plotted on (a) log and (b) linear scales. The PDF's by the p model (dotted line) are compared with the PDF's by the harmonious representation (solid line). Comparisons are displayed in pairs. The solid lines in each set of pairs are the same. For better visibility, each PDF is shifted by -2 unit in (a) and by -0.2 in (b) along the vertical axis. Parameters are given in the text.

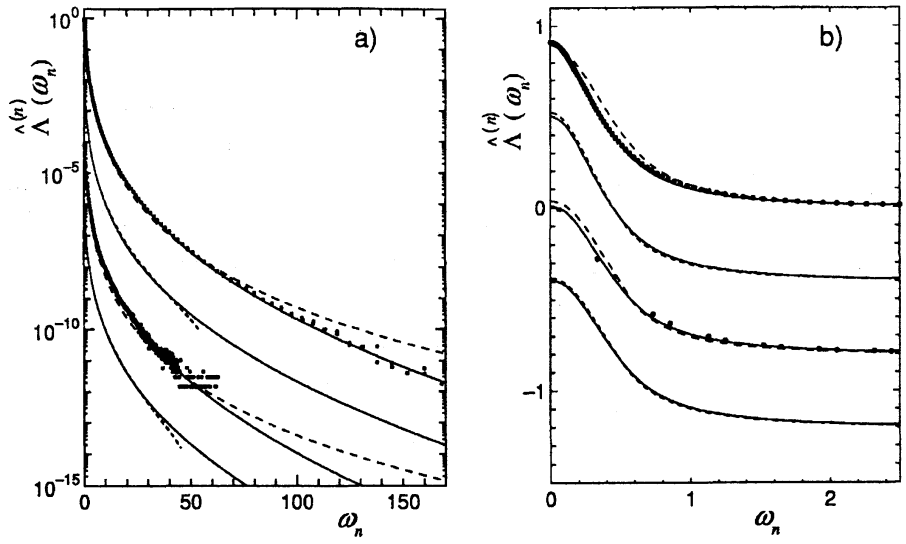

Figure 6: Analyses of the PDF's of *fluid particle accelerations*, measured by Gotoh et al. at $R_\lambda = 380$ (circles in the top set) and by Bodenschatz et al. at $R_\lambda = 690$ (circled in the bottom set), by means of the PDF's $\hat{\Lambda}^{(n)}(\omega_n)$ by the harmonious representation (solid line) and by the log-normal model (dashed line) are plotted on (a) log and (b) linear scales. The PDF's by the p model (dotted line) are compared with the PDF's by the harmonious representation (solid line). Results are displayed in pairs. The solid lines in each set of pairs are the same. For better visibility, each PDF is shifted by -2 unit in (a) and by -0.4 in (b) along the vertical axis. Parameters are given in the text.

points are symmetrized by taking averages of the left and the right hand sides data. In each set, a comparison of the PDF of the harmonious representation (solid line) with the PDF of the p model (dotted line) is given. For the harmonious PDF's (solid line), $q = 0.391$ ($\mu = 0.240$), and, from the top set to the bottom set, $(n,\ q') = (20.7,\ 1.60)$, $(13.6,\ 1.50)$, $(6.10,\ 1.20)$, $\xi_n^* = 1.10, 1.23, 1.43$ ($\alpha^* = 1.07$) and $\xi_n^{\max} = 204, 38.2, 6.63$. For the PDF by the log-normal model (dashed line), from the top set to the bottom set, $(n,\ q') = (21.5,\ 1.70)$, $(13.0,\ 1.63)$, $(5.00,\ 1.24)$ and $\xi_n^* = 1.19, 1.34, 1.51$ ($\alpha^* = 1.06$). For the PDF by the p model (dashed line), from the top set to the bottom set, $(n,\ q') = (21.0,\ 1.60)$, $(13.0,\ 1.62)$, $(5.50,\ 1.20)$, $\xi_n^* = 1.06, 1.07, 1.55$ ($\alpha^* = 1.08$) and $\xi_n^{\max} = 19.3, 7.70, 3.31$. The tail of PDF of the p model stops at $\xi_n^{\max}$ which is smaller than the maximum value of measured data point for each measuring distance. Note that every PDF's are plotted on (a) log and (b) linear scales.

In Fig. 6, the PDF's of the *fluid particle accelerations* (closed circles) reported by Gotoh et al. at $R_\lambda = 380$ (top set) [22] and by Bodenschatz et al. at $R_\lambda = 690$ (bottom set) [23, 24, 25] are analyzed with the PDF's $\hat{\Lambda}^{(n)}(\omega_n)$ of the harmonious representation (solid line) and of the log-normal model (dashed line). The measured data points both on the left and right hand sides of the PDF's are shown altogether on one side by closed circles in the figure. In each set, a comparison of the PDF of the harmonious representation (solid line) with the PDF of the p model (dotted line) is given. For the harmonious PDF's (solid

line), from the top set of pairs to the bottom set, q =0.391, 0.391 (μ = 0.240, 0.240), (n, q') =(17.5, 1.70), (17.1, 1.45) ω_n^* = 0.622, 0.605 (α^* = 1.01, 1.01), and $\omega_n^{\max}$ = 2530, 2040. For the PDF by the log-normal model (dashed line), from the top set to the bottom set, (n, q') = (17.0, 1.50), (18.5, 1.04), ω_n^* = 0.644, 0.558 (α^* = 1.00, 1.00), and $\omega_n^{\max}$ = 49.6, 76.6. For the PDF by the p model (dotted line), from the top set to the bottom set, (n, q') = (19.0, 1.50), (18.5, 1.20) ω_n^* = 0.539, 0.547 (α^* = 1.01, 1.01), and $\omega_n^{\max}$ = 54.1, 45.2. Note that every PDF's are plotted on (a) log and (b) linear scales.

The values of n for all the PDF's are determined by MLS by adjusting the integrand $\xi_n^4 \Pi_\phi^{(n)}(\xi_n)$ of the fourth moment both of data and of the theories. The values of q' for all the PDF's are obtained by MLS by fitting the theoretical PDF's at the center part, $|\xi_n| \leq \xi_n^*$, with the observed PDF's.

References

[1] A.M. Oboukhov: J. Fluid Mech. **13**, 77 (1962)

[2] A.N. Kolmogorov: J. Fluid Mech. **13**, 82 (1962)

[3] A.M. Yaglom: Sov. Phys. Dokl. **11**, 26 (1966)

[4] C. Meneveau, K.R. Sreenivasan: Phys. Rev. Lett. **59**, 1424 (1987)

[5] C. Meneveau, K. R. Sreenivasan: Nucl. Phys. B (Proc. Suppl.) **2**, 49 (1987)

[6] T. Arimitsu, N. Arimitsu: Phys. Rev. E **61**, 3237 (2000)

[7] T. Arimitsu, N. Arimitsu: J. Phys. A: Math. Gen. **33**, L235 (2000) [CORRIGENDUM: **34**, 673 (2001)]

[8] T. Arimitsu, N. Arimitsu: Chaos, Solitons and Fractals **13**, 479 (2002)

[9] T. Arimitsu, N. Arimitsu: Prog. Theor. Phys. **105**, 355 (2001)

[10] T. Arimitsu, N. Arimitsu: Physica A **295**, 177 (2001)

[11] N. Arimitsu, T. Arimitsu: J. Korean Phys. Soc. **40**, 1032 (2002)

[12] T. Arimitsu, N. Arimitsu: Physica A **305**, 218 (2002)

[13] T. Arimitsu, N. Arimitsu:t J. Phys.: Condens. Matter **14**, 2237 (2002)

[14] N. Arimitsu, T. Arimitsu: Europhys. Lett. **60**, 60 (2002)

[15] T. Arimitsu, N. Arimitsu: Condensed Matter Phys. (Lviv, Ukrain), **6**, 85 (2003)

[16] T. Arimitsu, N. Arimitsu: Physica D (2002) in press [cond-mat/0210274]

[17] T. Arimitsu, N. Arimitsu: cond-mat/0301516 (2003)

[18] T. Arimitsu and N. Arimitsu, In *Highlights in Condensed Matter Physics*, editors, C. Noce A. Avella, R. Citro and M. Salerno (AIP Conference Proceedings **695**, 2003) pp 135

[19] T. Arimitsu, N. Arimitsu: cond-mat/0312143 (2003)

[20] N. Arimitsu, T. Arimitsu: cond-mat/0312164 (2003)

[21] T. Gotoh, D. Fukayama, T. Nakano: Phys. Fluids **14**, 1065 (2002)

[22] T. Gotoh, private communication

[23] A. La Porta, G. A. Voth, A. M. Crawford et al: Nature **409**, 1017 (2001)

[24] G. A. Voth, A. La Porta, A. M. Crawford et al: J. Fluid Mech. **469**, 121 (2002)

[25] A. M. Crawford, N. Mordant and E. Bodenschatz, (2002) physics/0212080.

[26] S. S. Moiseev, A. V. Tur and V. V. Yanovskii, Sov. Phys. JETP **44** (1976) 556.

[27] U. Frisch and G. Parisi, In *Turbulence and Predictability in Geophysical Fluid Dynamics and Climate Dynamics*, editors, M. Ghil, R. Benzi and G. Parisi (North-Holland, New York 1985) pp 84

[28] R. Benzi, G. Paladin, G. Parisi and A. Vulpiani, J. Phys. A: Math. Gen. **17**, 3521 (1984)

[29] A. Rényi: *Proc. 4th Berkeley Symp. Maths. Stat. Prob.* **1**, 547 (1961)

[30] C. Tsallis: J. Stat. Phys. **52**, 479 (1988)

[31] J.H. Havrda, F. Charvat: Kybernatica **3**, 30 (1967)

[32] U.M.S. Costa, M.L. Lyra, A.R. Plastino et al: Phys. Rev. E **56**, 245 (1997)

[33] M.L. Lyra, C. Tsallis: Phys. Rev. Lett. **80**, 53 (1998)